Radiomics-based prediction of hemorrhage expansion among patients with thrombolysis/thrombectomy related–hemorrhagic transformation using machine learning

Junfeng Liu* iD **, Wendan Tao*, Zhetao Wang, Xinyue Chen, Bo Wu and Ming Liu**

Abstract

Introduction: Patients with hemorrhagic transformation (HT) were reported to have hemorrhage expansion. However, identification these patients with high risk of hemorrhage expansion has not been well studied.

Objectives: We aimed to develop a radiomic score to predict hemorrhage expansion after HT among patients treated with thrombolysis/thrombectomy during acute phase of ischemic stroke.

Methods: A total of 104 patients with HT after reperfusion treatment from the West China hospital, Sichuan University, were retrospectively included in this study between 1 January 2012 and 31 December 2020. The preprocessed initial non-contrast-enhanced computed tomography (NECT) imaging brain images were used for radiomic feature extraction. A synthetic minority oversampling technique (SMOTE) was applied to the original data set. The after-SMOTE data set was randomly split into training and testing cohorts with an 8:2 ratio by a stratified random sampling method. The least absolute shrinkage and selection operator (LASSO) regression were applied to identify candidate radiomic features and construct the radiomic score. The performance of the score was evaluated by receiver operating characteristic (ROC) analysis and a calibration curve. Decision curve analysis (DCA) was performed to evaluate the clinical value of the model.

Results: Among the 104 patients, 17 patients were identified with hemorrhage expansion after HT detection. A total of 154 candidate predictors were extracted from NECT images and five optimal features were ultimately included in the development of the radiomic score by using logistic regression machine-learning approach. The radiomic score showed good performance with high area under the curves in both the training data set (0.91, sensitivity: 0.83; specificity: 0.89), test data set (0.87, sensitivity: 0.60; specificity: 0.85), and original data set (0.82, sensitivity: 0.77; specificity: 0.78). The calibration curve and DCA also indicated that there was a high accuracy and clinical usefulness of the radiomic score for hemorrhage expansion prediction after HT.

Conclusions: The currently established NECT-based radiomic score is valuable in predicting hemorrhage expansion after HT among patients treated with reperfusion treatment after ischemic stroke, which may aid clinicians in determining patients with HT who are most likely to benefit from anti-expansion treatment.

Keywords: hemorrhage expansion, hemorrhagic transformation, machine learning, radiomic score, thrombolysis/thrombectomy

Correspondence to:
Ming Liu
Center of Cerebrovascular
Diseases, Department
of Neurology, West
China Hospital, Sichuan
University, No. 37 Guo Xue
Xiang, Chengdu 610041,
China
wyplmh@hotmail.com

Junfeng Liu
Wendan Tao
Bo Wu
Center of Cerebrovascular
Diseases, Department
of Neurology, West
China Hospital, Sichuan
University, Chengdu, China

Zhetao Wang
Department of Radiology,
West China Hospital,
Sichuan University,
Chengdu, China

Xinyue Chen
CT collaboration, Siemens
Healthineers,China

*The first two authors
contribute equally to this
study.

Introduction

Hemorrhagic transformation (HT) is the most feared complication of intravenous thrombolytic therapy and mechanical thrombectomy after ischemic stroke.[1] Previous studies[2–4] reported that HT is associated with poor outcomes, especially symptomatic HT that has a mortality rate approaching 50% and significant morbidity with survival. Treatment approaches in these patients showed substantial variability across different studies,[5–7] and no established treatment has been recommended by current guidelines.

Hemorrhage expansion has been reported in patients diagnosed with symptomatic HT, and it occurs in 30% to 40% of patients.[5–7] It suggests a therapeutic opportunity exists in those patients. Theoretically, the risk of hemorrhage expansion may be greater in patients with asymptomatic HT who received reperfusion treatment, especially in patients with successful recanalization or with endothelial injury related to a neuro-interventional procedure.[8] Given the high risk of ongoing bleeding after HT, early identification of patients with a potential risk of hemorrhage expansion is a potential target for therapeutic strategies.

The predictors and outcomes of hemorrhage expansion after HT have not been well studied. Prior studies[5–7] of hemorrhage expansion after thrombolysis only included patients with symptomatic HT and thus are weighted toward parenchymal hematoma (PH)-2. Recently, radiomic analysis was developed as a promising quantitative method for the objective assessment of the heterogeneity within lesions, which can capture image information not assessable by human eyes.[9,10] It has been proven to have a superior ability in prediction of extra-organ metastasis for cancers,[11,12] and hemorrhage expansion after spontaneous intracerebral hemorrhage.[13,14]

In this study, we hypothesized that extraction of quantitative radiomic image features on non-contrast-enhanced computed tomography (NECT) scans and evaluation of these data by an automated machine learning methods might offer additional information in the prediction of hemorrhage expansion after HT. To test and evaluate this hypothesis, we aimed to develop a quantitative radiomic score to predict hemorrhage expansion in patients diagnosed with HT on NECT brain scans after thrombolysis and/or thrombectomy. Furthermore, we investigated whether the radiomic model could predict the functional outcomes at 3 months after stroke onset.

Methods

Study participants

Participants were retrospectively retrieved from the Chengdu Stroke Registry,[15] which prospectively and consecutively included patients with stroke admitted to the department of neurology of West China Hospital since 2002. The study was approved by the Biomedical Research Ethics Committee of West China Hospital, Sichuan University (2016(339)). The need for patient consent for the present analysis was waived owing to its retrospective nature.

In the present study, patients with HT after thrombolysis and/or thrombectomy for current stroke treated within 6 hours after stroke onset between 1 January 2012 and 31 December 2020 were included. The exclusion criteria were the following conditions: (1) patients with HT were only detected on MRI; (2) patients received surgical decompressive craniotomy or hematoma evacuation after HT; (3) images contained severe artifacts; (4) intraventricular hemorrhage, subarachnoid hemorrhage, or remote intracerebral hemorrhage is involved; and (5) patients had no brain computed tomography (CT) scans for hemorrhage expansion assessment after HT diagnosis.

HT was defined as hemorrhage within the infarct territory which was detected on the follow-up brain CT scans during hospitalization, but not on the baseline admission scan. The median hospital stay was 15 days [interquartile range (IQR): 9–25 days]. The median time from stroke onset to HT detection was 2 days (IQR: 1–5 days). HT was defined as symptomatic HT according to the Neurological Disease and Stroke study.[4] HT was also classified as hemorrhagic infarction (HI)-1, HI-2, and PH-1, and PH-2 according to the European Cooperative Acute Stroke Study III definition.[16]

Demographic, vascular risk factor, and other clinical variables collection

Demographic and medical history including age, sex, hypertension, diabetes mellitus, atrial fibrillation, hyperlipidemia, previous stroke, smoking, and alcohol consumption were obtained from the

Chengdu stroke registry. Treatment before stroke (antiplatelet and anticoagulation), blood pressure on admission, initial National Institute of Health Stroke Scale (NIHSS) score, and blood glucose level were obtained from medical history records.

Qualitative neuroimaging predictors

All patients underwent an initial CT scan on admission, followed by a routine brain CT within 24 hours before starting anti-thrombotic therapy or a repeated CT immediately whenever hemorrhage was suspected, such as in the case of headache or neurological deterioration. When patients were diagnosed with HT on brain CT, three other imaging markers were also evaluated including the midline shift, the extent of hypodensity in the middle cerebral artery (MCA) territory, and the location of infarction. The Midline shift was defined as midline shift of more than 5 mm at the septum pellucidum level or more than 2 mm at the pineal gland level.[17] The extent of hypodensity was classified as whether or not the visible hypodensity involved $> 1/3$ of the MCA territory. The location of infarction was classified into anterior circulation infarction, posterior circulation infarction, or both anterior and posterior circulation infarction.

Image data acquisition and post-acquisition processing

All NECT images were carried out on SIEMENS SOMATOM definition CT scanner. The scanning was performed using a standard clinical protocol with an axial technique of 2.4-mm section thickness and reconstruction interval, and with a scanning energy of 120 kVp tube voltage. The image matrix size was 512×512. The scan ranged from the skull base to the cranium, with a thickness of 3 mm per layer.

Segmentation of hemorrhage and radiomic feature extraction

All the brain CT images transferred from the picture archiving and communication system (PACS) were saved as DICOM files and were then loaded into a semi-automatic segmentation software (Radiomic, Siemens Healthineers, Beijing, China). All the images were analyzed by a neurologist with 3 years of experience, who was blinded to patients' clinical data, and manually delineated the volume regions of interest (VOIs) along the hemorrhage boundary in multiple successive slices. We set each image to a window width of 80 HU and a window level of 35 HU as regular evaluation strategy.

VOIs were resampled to $1 \times 1 \times 1$ mm isotropic resolution using sitk BSpline. Subsequently, the same prototype (Radiomic, Siemens Healthineers) interfacing with the PyRadiomic was used for feature computation. All pixel gray levels inside the VOI objects were extracted for radiomic analysis. In total, 1691 quantitative image features were extracted for each VOIs. The extracted features included 324 first-order features, 17 shape features, 252 gray level dependence matrix (GLDM) features, 432 gray level co-occurrence matrix (GLCM) features, 288 gray level run length matrix (GLRLM) features, 288 gray level size zone matrix (GLSZM) features, and 90 neighboring gray tone difference matrix (NGTDM) features.

Outcomes

The primary outcome was hemorrhage expansion, defined as a 33% increase in the hematoma volume using the $(A \times B \times C)/2$ method on follow-up imaging. The secondary outcomes were 3-month mortality and 3-month mortality/disability, based on medical records or the interview with a relative. Mortality/disability was defined as a score of 3 to 6 on the modified Rankin Scale (mRS) at 3 months after stroke onset.

Model construction

Data splitting and pre-process

To eliminate the side effect of class imbalance on the modeling, synthetic minority oversampling technique (SMOTE) was applied to the original data set. Then the after-SMOTE data set was randomly split into training and testing cohorts with an 8:2 ratio by stratified random sampling method. And matched outcome distributions between cohorts was achieved. Before modeling, unsupervised feature selection methods were applied using training cohorts. Features with zero variance were eliminated. Besides collinearity between features were also checked. And algorithm was performed to eliminate minimal number of features to achieve all the pairwise correlations less than 0.75. In the end, 154 candidate features were included for the analysis.

Feature selection and modeling

Outcome-relevant features were selected based on the least absolute shrinkage and selection operator (LASSO) regression model using training cohorts after pre-process. Specifically, the tuning parameter of lambda was tuned by 5 repeats five cross-validation between multiple values from 0.01 to 2. The value of lambda with highest diagnostic ability was determined as for the model. Then the importance of features in differentiation based on this model was ranked. To balance between the complexity and accuracy of the model, only the top 5 features in this ranking list were enrolled in the final logistic regression model. Figure 1 described the model construction process.

Model performance

The logistic model using the top 5 features was evaluated in both training and testing cohorts. The receiver operator curves were drawn. And the area under these curves together with sensitivity, specificity, and accuracy using 0.5 as cutoff value for the model predicted probability were calculated as ways for calculation of apparent diagnostic ability of the model. In addition, the original sample were also used for model performance evaluation. Worth noting, as a way to estimate the stability and out-of-bag error of our model trained by small sample, the model was also tested in five resamples by bootstrapping of original data. Calibration curve was also performed to visually assess the agreement between model predictive and actual probability for original data set. Then decision curve analysis (DCA) was used to evaluate the clinical value of the radiomic model independently on the basis of calculating the net benefit for patients at each threshold probability.

After acquiring the model predictive probability for each sample in the original data set, the predictive probability was also used to predict 3-month death and 3-month death/disability. And its ability in the prognosis prediction was also evaluated in terms of receiver operator curve (ROC) with area under curve (AUC).

Statistical analysis

All clinical variables were compared between groups by using *t* test, Kruskal-Wallis test, chi-squared test, and Fisher exact, accordingly. All analyses were conducted by using the R statistical programming environment (version 3.4.3. http://www.R-project.org). A *p* value < 0.05 was considered to indicate a significant difference.

Data availability

The data that support the findings of this study are available from the corresponding author on reasonable request.

Results

Study participants and baseline characteristics

A total of 104 patients were finally included in the present study between 1 January 2012 and 31 December 2020 (Supplemental Figure I). The mean age was 68.2 ± 15 years, and 59 (56.9%) were male. Seventeen patients were identified with hemorrhage expansion after HT diagnosis. The median time from stroke onset to HT detection was 2 days (IQR: 1–5 days) and the median time from HT detection to hemorrhage expansion was 4 days (IQR: 1–5 days). The baseline demographic, clinical, and imaging characteristics are presented in Table 1.

No significant differences ($p > 0.05$) were found in all baseline clinical features between patients with and without hemorrhage expansion. Patients with hemorrhage expansion had a modestly higher initial NIHSS score (median: 18 *versus* 16, $p = 0.06$), though not significant. Similarly, no statistically significant differences of imaging characteristics were observed between patients with and without hemorrhage expansion.

Radiomic features selection

We applied SMOTE to generate a more balanced data set, resulting in 51 patients with hemorrhage expansion compared with 68 patients without hemorrhage expansion. In the SMOTE data set, 80% (96 patients) were randomly selected as a training cohort, and 20% (23 patients) as a testing cohort.

A total number of 154 predictors were included for evaluating the importance of predicting hemorrhage expansion. And best tuned lambda for the trained LASSO was 0.0148 by the training cohort (Figure 2).
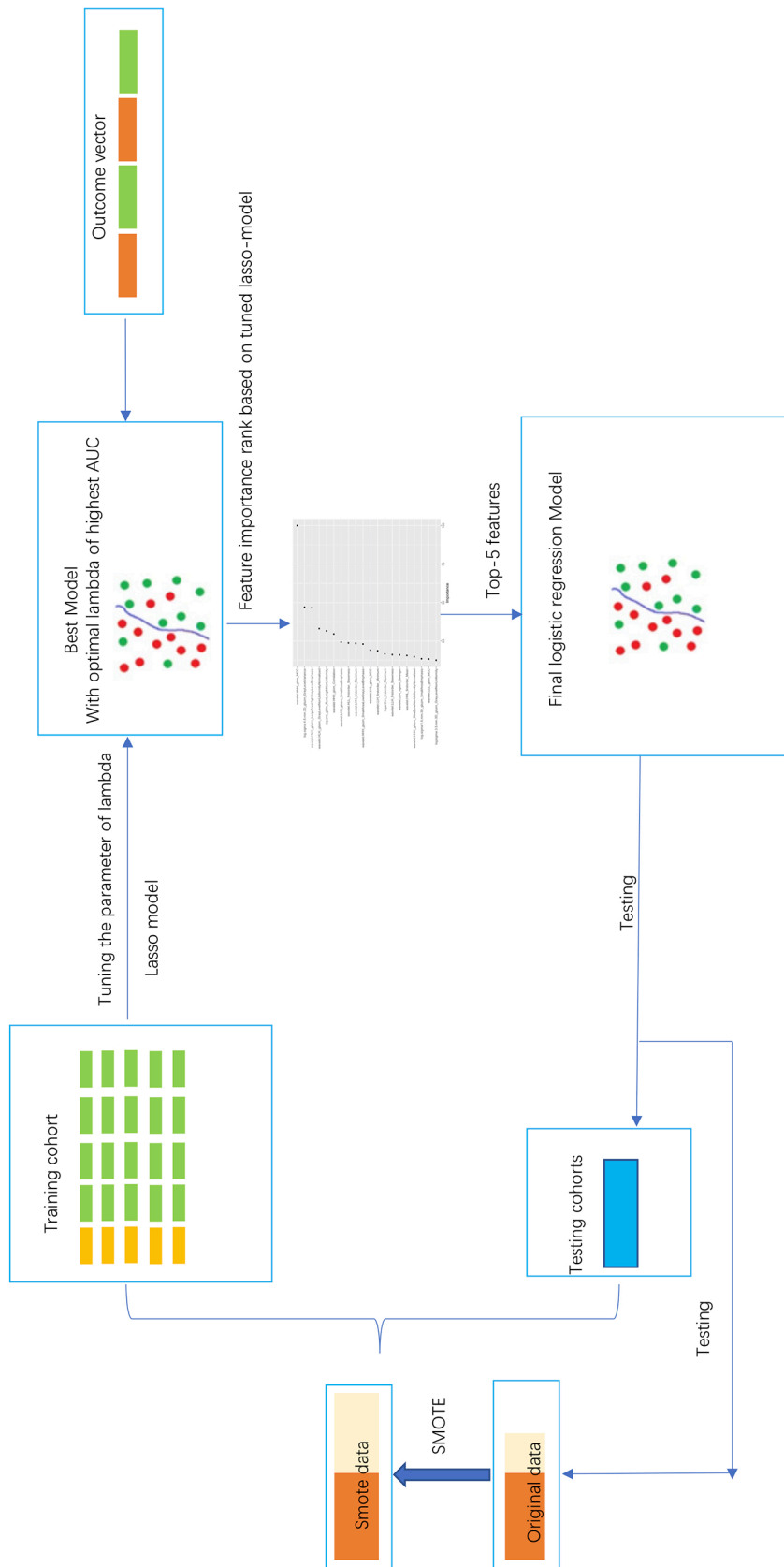
Figure 1. The radiomic score construction process.

Table 1. Baseline demographic, clinical, and radiological characteristics.

Variables	All (*n* = 104)	Without hematoma expansion (*n* = 87)	With hematoma expansion (*n* = 17)	*p*
Demographic variables				
Age, mean (SD)	68.23 (15.02)	67.39 (15.54)	72.53 (11.43)	0.20
Male, *n* (%)	59 (56.7)	52 (59.8)	7 (41.2)	0.19
Clinical variables				
OTT, median (IQR), hours	3.00 [2.00, 4.00]	3.00 [2.04, 4.00]	4.00 [2.00, 4.00]	0.77
Time to HT detection, median (IQR), days	1.51 [1.09, 4.86]	1.74 [1.12, 4.63]	1.14 [0.98, 6.67]	0.38
Length of stay, median (IQR), days	15.00 [9.00, 25.00]	15.00 [10.00, 25.00]	14.00 [4.00, 19.00]	0.17
NIHSS score on admission, median (IQR)	16.00 [12.00, 20.00]	16.00 [12.00, 19.00]	18.00 [16.00, 22.00]	0.06
Systolic blood pressure, mean (SD)	142.07 (25.69)	142.63 (25.10)	139.18 (29.17)	0.61
Diastolic blood pressure, mean (SD)	81.71 (15.13)	82.83 (15.39)	76.00 (12.66)	0.09
Glucose on admission, mean (SD)	8.14 (2.19)	8.20 (2.27)	7.79 (1.76)	0.48
Hypertension, *n* (%)	59 (56.7)	49 (56.3)	10 (58.8)	0.85
Diabetes, *n* (%)	25 (24.0)	19 (21.8)	6 (35.3)	0.23
Hyperlipidemia, *n* (%)	4 (3.8)	4 (4.6)	0 (0.0)	0.37
Atrial fibrillation, *n* (%)	49 (47.1)	39 (44.8)	10 (58.8)	0.30
Previous stroke, *n* (%)	11 (10.6)	10 (11.5)	1 (5.9)	0.69
Smoking, *n* (%)	35 (33.7)	32 (36.8)	3 (17.6)	0.17
Drinking, *n* (%)	27 (26.0)	23 (26.4)	4 (23.5)	0.80
Previous antiplatelets, *n* (%)	5 (4.8)	5 (5.7)	0 (0.0)	0.59
Previous anticoagulation, *n* (%)	8 (7.7)	6 (6.9)	2 (11.8)	0.61
Cardioembolic stroke, *n* (%)	58 (55.8)	48 (55.2)	10 (58.8)	0.78
Imaging variables				
ECASS classification				0.64
HI-1, *n* (%)	2 (1.9)	2 (2.3)	0 (0.0)	
HI-2, *n* (%)	17 (16.3)	16 (18.4)	1 (5.9)	
PH-1, *n* (%)	50 (48.1)	41 (47.1)	9 (52.9)	
PH-2, *n* (%)	35 (33.7)	28 (32.2)	7 (41.2)	
Symptomatic HT, *n* (%)	37 (35.6)	28 (32.2)	9 (52.9)	0.16
Location of infarction, *n* (%)				0.95
Anterior	94 (90.4)	79 (90.8)	15 (88.2)	
Posterior	5 (4.8)	4 (4.6)	1 (5.9)	
Anterior + Posterior	5 (4.8)	4 (4.6)	1 (5.9)	
Midline shift, *n* (%)	43 (41.3)	35 (40.2)	8 (47.1)	0.60
> 1/3 middle cerebral artery territory, *n*(%)	78 (75.0)	64 (73.6)	14 (82.4)	0.55

ECASS, European Cooperative Acute Stroke Study; HI-1, hemorrhagic infarction-1; HI-2, hemorrhagic infarction-2; HT, hemorrhagic transformation; IQR, interquartile range; NIHSS, National Institute of Health Stroke Scale; OTT, onset to treatment time; PH-1, parenchymal hematoma-1; PH-2, parenchymal hematoma-2; SD, standard deviation.
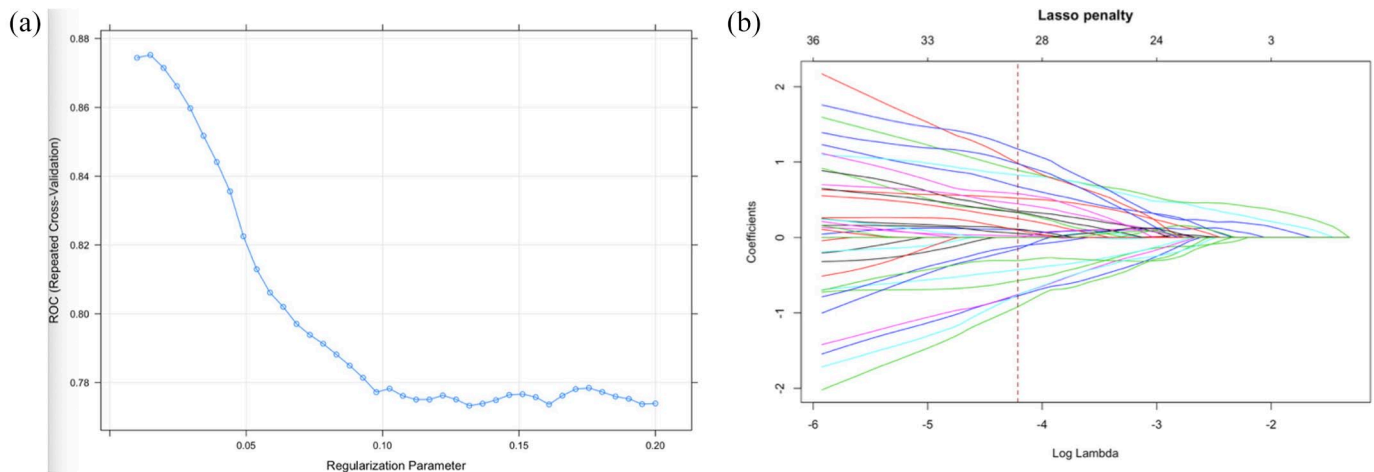
(a)

(b)

Figure 2. Radiomics feature selection using the least absolute shrinkage and selection operator (LASSO) binary logistic regression model. (a) Tuning parameter (λ) selection in the LASSO model used 5 repeats 5-fold cross-validation. The area under the curves (AUC) was plotted versus log (λ). (b) LASSO coefficient profiles (y-axis) of the selected features. The upper and lower x-axis represented the feature number and the log (λ), respectively. The dashed vertical line was drawn at the optimal lambda value of 0.0148.

Radiomic score building and its performance for predicting hemorrhage expansion

To reduce the redundancy and unnecessary complexity of the radiomic score, the top 5 features (log.sigma.2.5.mm.3D_firstorder_90Percentile, wavelet.LLH_firstorder_Kurtosis, wavelet.HHL_gldm_GrayLevelVariance,wavelet.LHH_first order_Skewness,log.sigma.1.5.mm.3D_glszm_LowGrayLevelZoneEmphasis) were retained for developing radiomic score (the definition of the features can be found at https://pyradiomics.readthedocs.io/en/latest/). The distribution of the five features is presented in Figure 3.

Five-fold five cross-validation was carried out to tune these features of the classifier during the training procedure using. These features were constructed for the radiomic score using logistic regression algorithm and the calculation formula was as follows: $y = -1.43 + (-1.81 \times$ log.sigma.2.5.mm.3D_firstorder_90 Percentile) + $(1.42 \times$ wavelet.LLH_firstorder_Kurtosis) + $(-1.29 \times$ wavelet.HHL_gldm_GrayLevel Variance) + $(-1.43 \times$ wavelet.LHH_firstorder_Skewness) + $(0.94 \times$ log.sigma.1.5.mm.3D_glszm_LowGrayLevelZoneEmphasis). The performance evaluation was conducted by using the AUC analysis, and the results were shown in Table 2/supplementary Figure II. The apparent AUC for the radiomic score on the training cohort was 0.91 [95% confidence interval (CI) 0.84–0.97], 0.87 (95% CI 0.72–1.00) for testing cohort, and 0.85 (95% CI: 0.76–0.93) for original data set.

In regard to the internal validation for the radiomic score predicting hemorrhage expansion, we also observed a good performance, and the results of five resamples by bootstrapping of original data were presented in supplementary Figure II-D. The mean AUC was 0.93 and it suggested that our radiomic score is relatively reliable and stable. Figure 4(a) illustrates the calibration curve of the radiomic score based on the original data set, which suggested a favorable predictive performance satisfactorily consistent with the ideal curve. In addition, decision curve analysis was conducted to assess the clinical utility of the radiomic score (Figure 4(b)). The decision curve demonstrated that intervention on patients with HT on the basis of the radiomic model leads to higher benefit.

Performance of the radiomic score predicting 3-month death and death/disability

In our cohort, none of the 104 patients were lost to follow-up at 3 months. The 3-month death and death/disability were 18.3% (19/104) and 64.4% (67/104), respectively. A good performance for predicting 3-month death (AUC, 0.67; 95% CI, 0.54–0.80), and 3-month death/disability (AUC,
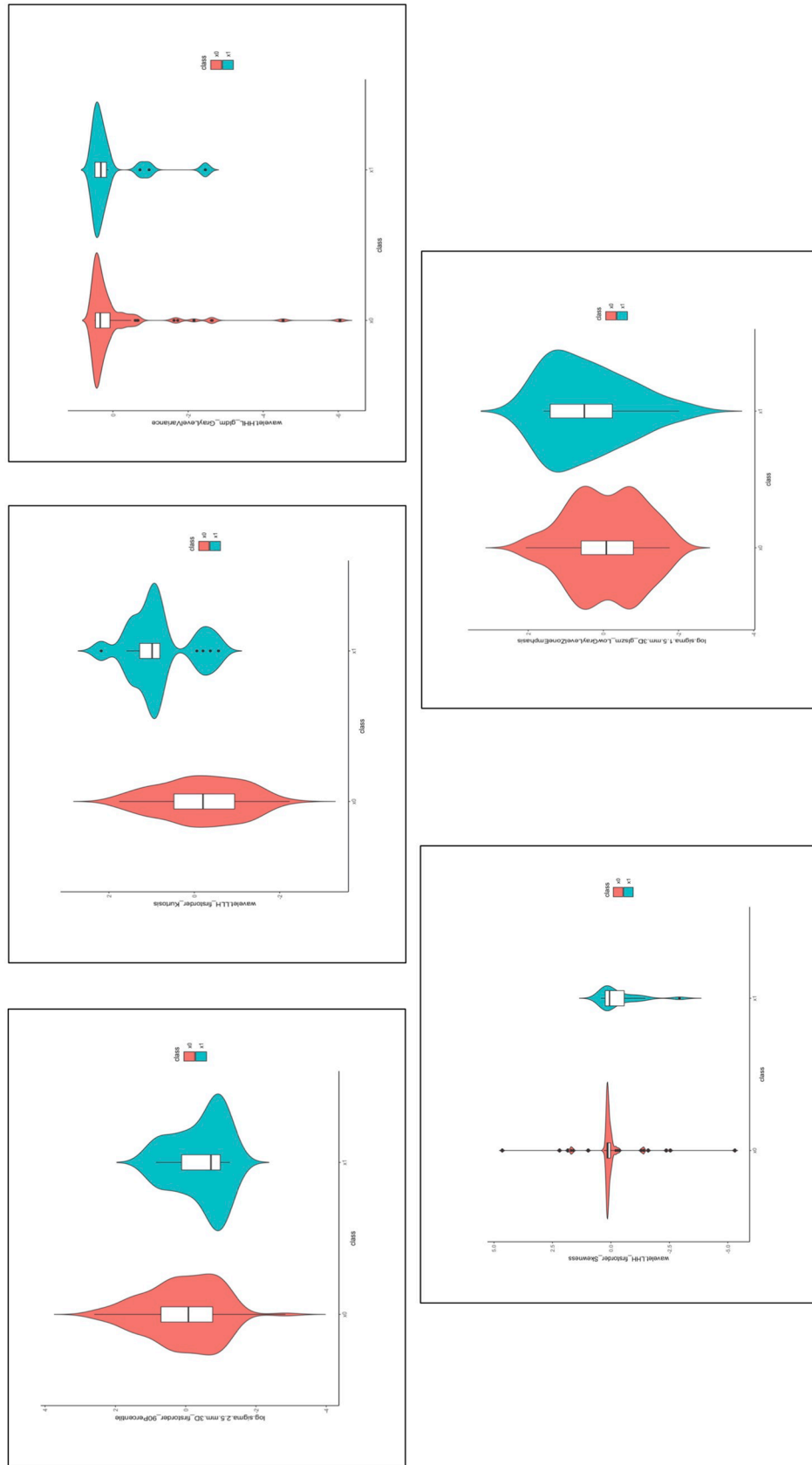
Figure 3. The distribution of the 5 radiomic features in the SMOTE data set. Red means patients without hemorrhage expansion; blue means patients with hemorrhage expansion.

Table 2. Predictive performance of radiomic models on the risk of hematoma expansion.

	AUC (95% CI)	Sensitivity	Specificity	Accuracy
SMOTE data set (n = 119)				
Training cohort (n = 96)	0.91 (0.84–0.97)	0.83	0.89	0.87
Testing cohort (n = 23)	0.87 (0.73–1.00)	0.60	0.85	0.74
Original data set (n = 109)	0.85 (0.76–0.93)	0.82	0.77	0.78

AUC, area under curve; CI, confidence interval; SMOTE, synthetic minority oversampling technique.
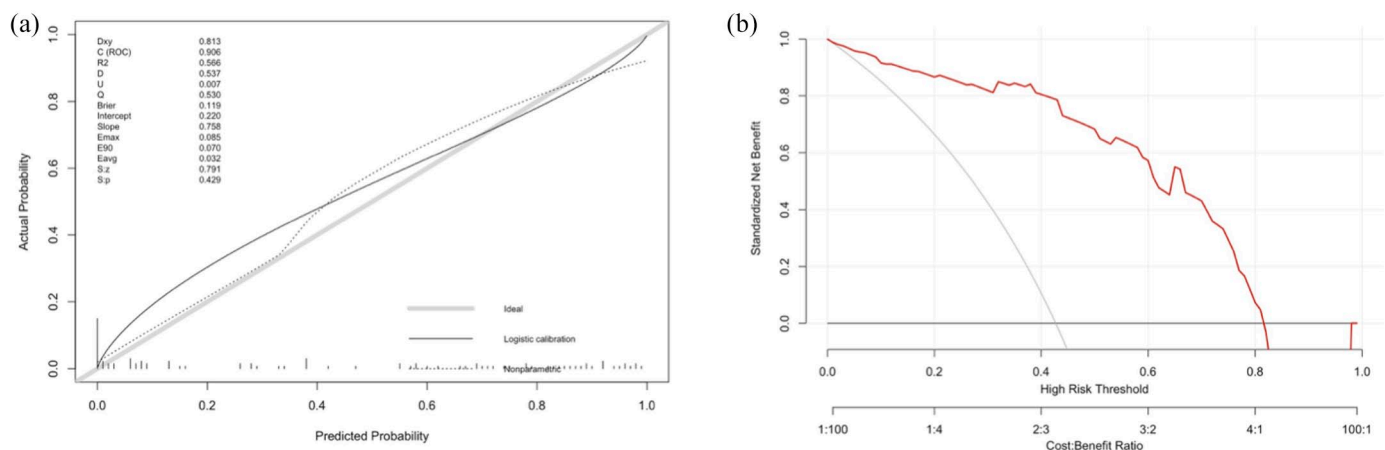
Figure 4. Calibration curve and decision curve analysis of the radiomic score. (a) Calibration curve of the radiomic score. (b) Decision curve analysis for radiomic score. The red line indicates the decision curve of the radiomic score. The y-axis measures the net benefit; the x-axis represents the predictive probability threshold.

0.63; 95% CI, 0.52–0.75) was also observed in the study, which suggested the prognostic value of the radiomic score. In addition, the radiomic score was also significantly associated with an increased risk of 3-month death (unadjusted OR, 5.17; 95% CI, 1.36–20.81, p = 0.02), and 3-month death/disability (unadjusted OR, 4.70; 95% CI, 1.40–18.12, p = 0.02).

Discussion

The present study developed a predictive model for hemorrhage expansion after HT incorporating five robust radiomic features which were extracted from NECT brain images, and the radiomic score showed a good performance with good discrimination and calibration. To our knowledge, the present study is the first study to develop a proposed machine learning algorithm using quantitative radiomic features derived from NECT brain scans for predicting hemorrhage expansion after

HT among ischemic stroke patients who received reperfusion treatment.

In the construction of the radiomic score, five radiomic features belonging to first order (90 Percentile, Kurtosis, and Skewness), gldm (Gray Level Variance), and glszm (Low Gray Level Zone Emphasis) features, which described intensity, texture, and heterogeneity, were finally selected from 154 candidate features. The more active and fresh bleeding points in the hemorrhage, the more hypo-attenuation regions on CT, and the greater heterogeneity of the hemorrhage, all of which predicted a tendency of hemorrhage expansion.

In our study, none of the clinical variables and qualitative imaging markers (such as symptomatic HT, HI-1, HI-2, PH-1, and PH-2) were found to be associated with hemorrhage expansion. In recent years, a growing number of imaging

markers for predicting spontaneous intracerebral hemorrhage expansion such as the swirl sign, blend sign, and island sign have been investigated and proposed.[18–20] However, these markers may not be suitable for hemorrhage expansion after HT, considering the differences of radiographic appearance between HT and spontaneous intracerebral hemorrhage. Besides, most of the qualitative imaging markers are subjective, which could contribute to a discrepancy between observers. Therefore, instead of defining new qualitative imaging markers, more objective quantitative radiomic features based on NECT scans using machine learning algorithm may be a better way to predict hemorrhage expansion after HT. In addition, recent evidence[21,22] suggested that lots of biomarkers such as neutrophil-to-lymphocyte ratio and MMP-9 related to the risk of HT. Future studies with larger sample size were needed to investigate whether adding these biomarkers or clinical characteristics into our radiomic score could improve the ability of prediction hematoma expansion.

Hemorrhage expansion is a major predictor of death and disability in patients with intracerebral hemorrhage.[23–25] Similarly, we also found a good performance of the radiomic score for predicting 3-month death and death/disability. Therefore, prevention of hemorrhage expansion may be an important approach to improve the functional outcomes after HT. However, the current evidence did not show any efficacy of anti-expansion therapies in improving outcomes of HT. It seems like that a small proportion of patients with high risk of expansion may have an opportunity to clinically benefit from intensive therapies such as intensive blood pressure control, aggressive reversal of coagulopathy, and neurosurgical treatment. We think in the future our fast and easy to use radiomic score combining machine learning algorithm for hemorrhage expansion prediction after HT may play a role in personalized and tailored medicine on anti-expansion therapy. Moreover, another possible use of the radiomic score would be in the selection of patients for randomized trials on therapies to reduce the risk of expansion and improve the outcomes of HT.

There were some limitations of the currents study that still need to be further investigated. First, our study is limited by its retrospective design with a relatively small and imbalanced sample size, and the non-standardized timing of follow-up CT scans. In our center, a follow-up CT is performed based upon clinicians' preference or with neurological deterioration. In the future, prospective studies with a large sample size and standardized image acquisition are needed to verify the findings. Second, the established radiomic score lacks external validation. Despite that, the good performance in internal validation using bootstrapping method to some extent confirm the radiomic score's generalization and robustness. Third, despite the good performance of our radiomic score, it is not currently available for real-time application and would require significant further development and validation for clinical use. However, considering the rapid development of artificial intelligence, the application of the radiomic score in everyday clinical practice will come soon. Last, the hemorrhage density on CT scans could be affected by the time interval of stroke onset to HT detection. As hemorrhage density decreases over time, this might have biased results. However, no difference of the time from stroke onset to HT diagnosis between patients with and without hemorrhage expansion was found in the study.

Conclusions

In conclusion, the radiomic score established by using machine learning showed good performance in the prediction of hemorrhage expansion after HT among ischemic stroke patients treated with reperfusion therapy. The radiomic score may provide an individualized tool to identy patients with high risk of hemorrhage expansion after HT, and its favorable sensitivity and calibration may help clinicians select patients that are most likely to benefit from anti-expansion treatment and improve the long-term prognosis of patients with HT.

Author contribution
Junfeng Liu drafted the manuscript and analyzed the data. Wendan Tao and Zhetao Wang collected the data. Xinyue Chen performed the radiomic analysis. Bo Wu revised the manuscript. Ming Liu designed and supervised the research.

ORCID iD

Junfeng Liu (iD) https://orcid.org/0000-0002-3858-0763

Supplemental material

Supplemental material for this article is available online.

References

1. Álvarez-Sabín J, Maisterra O, Santamarina E, *et al.* Factors influencing haemorrhagic transformation in ischaemic stroke. *Lancet Neurol* 2013; 12: 689–705.

2. Fiorelli M, Bastianello S, von Kummer R, *et al.* Hemorrhagic transformation within 36 hours of a cerebral infarct: relationships with early clinical deterioration and 3-month outcome in the European Cooperative Acute Stroke Study I (ECASS I) cohort. *Stroke* 1999; 30: 2280–2284.

3. Berger C, Fiorelli M, Steiner T, *et al.* Hemorrhagic transformation of ischemic brain tissue asymptomatic or symptomatic? *Stroke* 2001; 32: 1330–1335.

4. National Institute of Neurological Disorders and Stroke rt-PA Stroke Study Group. Tissue plasminogen activator for acute ischemic stroke. The National Institute of Neurological Disorders and Stroke rt-PA Stroke Study Group. *N Engl J Med* 1995; 14: 1581–1587.

5. Goldstein JN, Marrero M, Masrur S, *et al.* Management of thrombolysis-associated symptomatic intracerebral hemorrhage. *Arch Neurol* 2010; 67: 965–969.

6. Alderazi YJ, Barot NV, Peng H, *et al.* Clotting factors to treat thrombolysis-related symptomatic intracranial hemorrhage in acute ischemic stroke. *J Stroke Cerebrovasc Dis* 2014; 23: e207–e214.

7. Yaghi S, Boehme AK, Dibu J, *et al.* Treatment and outcome of thrombolysis-related hemorrhage. *JAMA Neurol* 2015; 72: 1451–1457.

8. Yaghi S, Willey JZ, Cucchiara B, *et al.* Treatment and outcome of hemorrhagic transformation after intravenous alteplase in acute ischemic stroke a scientific statement for healthcare professionals from the American Heart Association/American Stroke Association. *Stroke* 2017; 48: e343–e361.

9. Kumar V, Gu Y, Basu S, *et al.* Radiomics: the process and the challenges. *Magn Reson Imaging* 2012; 30: 1234–1248.

10. Gillies RJ, Kinahan PE and Hricak H. Radiomics: images are more than pictures, they are data. *Radiology* 2016; 278: 563–577.

11. Davnall F, Yip CSP, Ljungqvist G, *et al.* Assessment of tumor heterogeneity: an emerging imaging tool for clinical practice. *Insights Imaging* 2012; 3: 573–589.

12. Hu TD, Wang SP, Huang L, *et al.* A clinical-radiomics nomogram for the preoperative prediction of lung metastasis in colorectal cancer patients with indeterminate pulmonary nodules. *Eur Radiol* 2019; 29: 439–449.

13. Chen Q, Zhu D, Liu J, *et al.* Clinical-radiomics nomogram for risk estimation of early hematoma expansion after acute intracerebral hemorrhage. *Acad Radiol* 2021; 28: 307–317.

14. Xu W, Ding Z, Shan Y, *et al.* A nomogram model of radiomics and satellite sign number as imaging predictor for intracranial hematoma expansion. *Front Neurosci* 2020; 14: 491.

15. Liu J, Zheng L, Cheng Y, *et al.* Trends in outcomes of patients with ischemic stroke treated between 2002 and 2016: insights from a Chinese cohort. *Circ Cardiovasc Qual Outcomes* 2019; 12: e005610.

16. de Los Ríos la Rosa F, Khoury J, Kissela BM, *et al.* Eligibility for intravenous recombinant tissue-type plasminogen activator within a population: the effect of the European Cooperative Acute Stroke Study (ECASS) III trial. *Stroke* 2012; 43: 1591–1595.

17. Delgado P, Sahuquillo J, Poca MA, *et al.* Neuroprotection in malignant MCA infarction. *Cerebrovasc Dis* 2006; 21: 99–105.

18. Li Q, Zhang G, Huang YJ, *et al.* Blend sign on computed tomography: novel and reliable predictor for early hematoma growth in patients with intracerebral hemorrhage. *Stroke* 2015; 46: 2119–2123.

19. Li Q, Liu QJ, Yang WS, *et al.* Island sign: an imaging predictor for early hematoma expansion and poor outcome in patients with intracerebral hemorrhage. *Stroke* 2017; 48: 3019–3025.

20. Al-Nakshabandi NA. The swirl sign. *Radiology* 2001; 218: 433.

21. Turner RJ and Sharp FR. Implications of MMP9 for blood brain barrier disruption and hemorrhagic transformation following ischemic stroke. *Front Cell Neurosci* 2016; 10: 56.

22. Świtońska M, Piekuś-Słomka N, Słomka A, *et al.* Neutrophil-to-lymphocyte ratio and symptomatic hemorrhagic transformation in ischemic stroke patients undergoing revascularization. *Brain Sci* 2020; 10: 771.

23. Brott T, Broderick J, Kothari R, *et al.* Early hemorrhage growth in patients with intracerebral hemorrhage. *Stroke* 1997; 28: 1–5.

24. Davis SM, Broderick J, Hennerici M, *et al.* Hematoma growth is a determinant of mortality and poor outcome after intracerebral hemorrhage. *Neurology* 2006; 66: 1175–1181.

25. Yaghi S, Dibu J, Achi E, *et al.* Hematoma expansion in spontaneous intracerebral hemorrhage: predictors and outcome. *Int J Neurosci* 2014; 124: 890–893.